CIRCE-THETIS FACILITY CFD SIMULATION: STEADY STATE AND TRANSIENT COMPLIANCE

MARIA MANUELA PROFIR and VINCENT MOREAU
CRS4, Science and Technology Park, Piscina Manna, 09050, Cagliari, Italy
e-mail: manuela@crs4.it

Abstract
CIRCE is a large scale LBE pool-type facility operated by ENEA (Italy), with the aim to support the development of the Liquid Metal Fast Reactors (LMFR), in particular of ALFRED design. The H2020 PATRICIA project foresees the installation in the CIRCE facility of a new test section, named THETIS. Investigation of the transition between forced and natural circulation under different and competitive heat removal mechanisms are foreseen. A CFD model of the test section able to simulate both steady state and the foreseen experimental transients is under construction. In the paper, the complete CFD model of the THETIS test section has been described. The thermal radiation influence wherever relevant was highlighted. Suitable thermal boundary conditions for the steady state were implemented. The numerical results of the nominal steady-state pre-test simulation were presented and the upgrade for the transient simulations has been discussed.

Keywords: CFD simulation, CIRCE, ALFRED, LMFR

Introduction

For the safety concerns, it is important to prove that natural circulation in a reactor can be achieved with the Decay Heat Removal (DHR) systems such that the core cooling is guaranteed. For this reason, in many European projects developed in the Euratom Program framework, much effort is put to investigate the transition from forced to natural circulation both in experimental facilities and in numerical simulations and to generate data for numerical models validation. Computational thermal-hydraulics and computational fluid-dynamics (CFD) are intensively used to capture flow patterns and temperature distributions of the coolant in the plenum on a fine and detailed scale thanks to the computational power increase and to the advancements in the numerical modelling.

This paper focuses on the modelling by CFD means of the CIRCE (CIRColazione Eutettico) heavy liquid-metal pool-type facility, operated by ENEA, Italy. The CIRCE facility uses Lead Bismuth Eutectic as coolant [1] and supports the development of LMFRs, in particular ALFRED (Advanced Lead-cooled Fast Reactor European Demonstrator) design, the European demonstrator of the GEN-IV power plants concept. During the European H2020 projects SESAME (thermal hydraulics Simulations and Experiments for the Safety Assessment of MEtal cooled reactors) and MYRTE (MYRRHA Research and Transmutation Endeavour), the CIRCE facility was operated first in its Integral Circulation Experiments (ICE) set-up [2, 3], and was successively refurbished with a dedicated test section named HERO (Heavy liquid mEtal–pRessurized water cOoled tube) [4-6]). Several experimental campaigns were performed, supported by thermal-hydraulics numerical analyses, to provide data for pool thermal-hydraulics assessment and to generate databases for CFD and STH models validation [7, 8].

In the framework of the ongoing PATRICIA (Partitioning And Transmuter Research Initiative in a Collaborative Innovation Action) project, the HERO test section is replaced by a new one called THETIS (Thermal-hydraulic HElical Tubes Innovative System) [9]. The new test section includes an innovative Helical-Coil Steam Generator (HCSG) [10] and a new circulation mechanical pump (MCP). In PATRICIA project, several transitions from forced to natural circulation with several DHR competitive mechanisms will be tested in the experimental campaign. The expected flow rate and the power extracted by the heat exchanger in forced circulation are 35 kg/s and 400-450 kW, respectively.

In this paper, the CFD model of CIRCE-THETIS facility, built by means of the STAR-CCM+ software [11] is discussed. First, the geometrical model of the experimental test section and the modelling strategies are presented, as well as several preliminary results of the nominal steady-state simulation. Then, the progressive improvements of the model are illustrated, regarding the Reactor Vessel Auxiliary Cooling System (RVACS) and the vessel insulation. Finally, suitable thermal boundary conditions for the steady state are implemented in the context of the thermal radiation model, and the heat losses are evaluated

CIRCE-THETIS experimental facility

CIRCE is a large scale pool-type facility, representative of a generic pool-type LMFR, in which several integral experiments has been performed [12]. The internal diameter of the CIRCE main vessel is 1200 mm, with a height of 8500 mm and a thickness of 15 mm; during operation, CIRCE works with about 70 tons of liquid LBE.

The new test section to be installed in the CIRCE vessel, the THETIS test section, is illustrated in Fig. 1 (left side) together with the main flow path [13]. THETIS test section will consist of the following main components: the *Fuel Pin Simulator* (FPS, in red) for the heating of the liquid metal, consisting in an electrical pins bundle (1 m active length) which provide a nominal power of ~1 MW; the *Fitting Volume* (FV, in green) which collects the hot LBE rising from the FPS and allows the hydraulic connection between the FPS and the Riser; the *Riser* (in orange) connecting FV with the pump, provided with a double wall air-filled pipe to prevent the heat losses from the riser to the pool; the *Main Circulation Pump* (MCP, in yellow) a centrifugal vertical pump meant to perform the circulation of the LBE in forced circulation regime; the *LBE Separator* (in gold) on the top which feeds the HCSG, collecting the hot LBE and allowing the separation of the

argon flowing into the cover gas and the LBE going downward into the heat exchanger; the *HCSG* (in blue) for the heat removal from the primary system; the *Dead Volume*, which encloses and maintains insulated the power supply rods feeding the FPS.

The main flow path in THETIS is given in the following. The LBE enters from the feeding conduit situated at the bottom part of the FPS and is heated by the electrical pin bundle. Then, it is collected in the fitting volume, from which it flows upward through the Riser and the pump suction; the pump pushes up the fluid into the separator (hot pool). From the separator, the hot LBE enters into the shell side of the HCSG, where it is cooled by secondary pressurized water flowing in the tube side of the helical tube bundle and is discharged into the main vessel, closing in this way the LBE primary loop inside the pool.
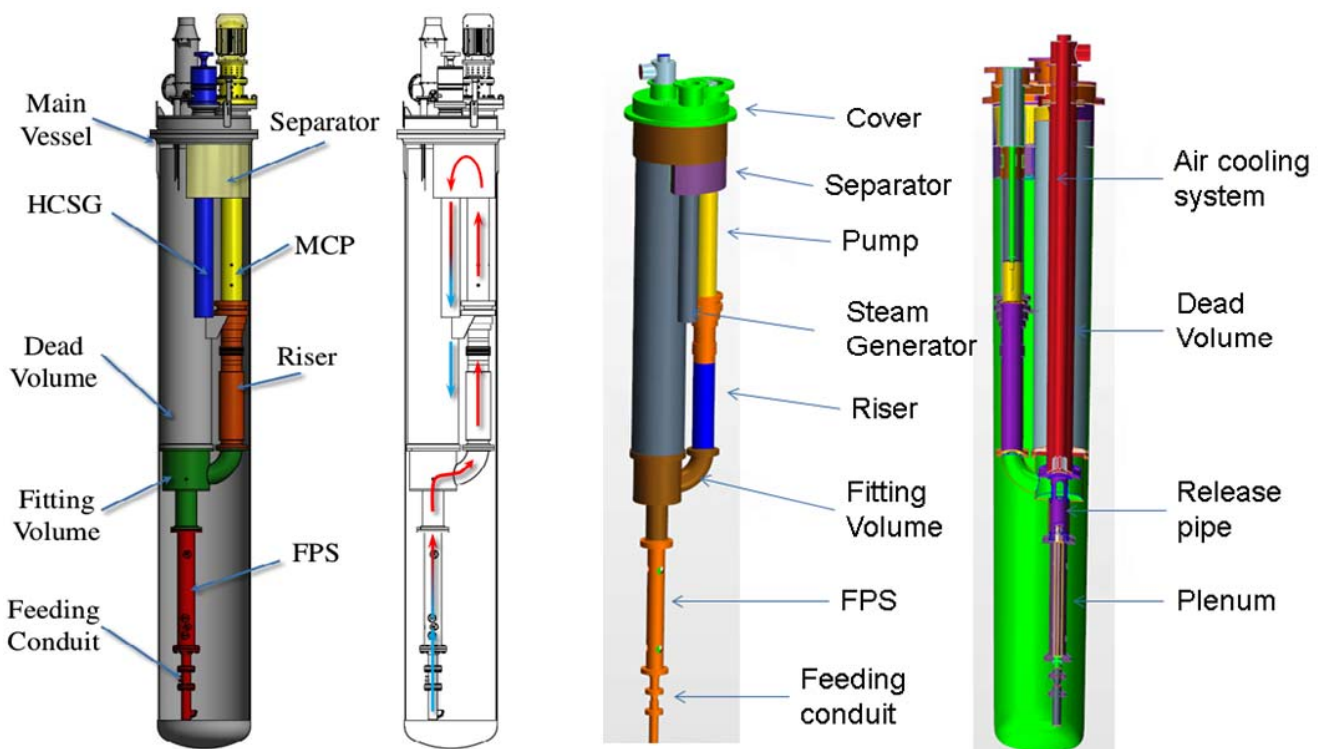
Fig.1 THETIS Test Section schematic view and flow path (left, courtesy of ENEA); CFD geometry (right)

CIRCE-THETIS STAR-CCM+ numerical model. Preliminary results

The THETIS test section numerical model built by using STAR-CCM+ software (versions 15 and 16) is described hereafter. Fig.1 illustrates the main components (in CAD geometry) of the CIRCE-THETIS model (right side), built with the 3D-CAD modeller embedded in STAR-CCM+. For an accurate representation of the local flow patterns in the plenum, which have an important influence on the wall heat fluxes, a high level of detail is necessary. Therefore, a particular effort has been done to build a quite detailed geometry. The fluid volumes included in the simulation (see Fig. 1, right side) are the following: the feeding conduit with a Venturi flow meter, the fuel pin bundle (with a simplified representation), the fitting volume, the riser, the pump, the separator (hot pool), the dead volume, the air cooling channel, the steam generator with two air

gaps (acting as thermal insulators) in the double wall shells, and the main pool. The main LBE volume is a single phase flow. The cover gas (Argon) is a separated region communicating by means of conducting baffle interfaces with the hot pool. The solid structures included successively are the feeding conduit, the FPS hexagonal wrapper and the release pipe, the fitting volume connected with the riser, the pump body, the dead volume with the air cooling assembly, the separator, the steam generator inner and outer shells, the tank, and the cover.

The electrical pins heating the LBE are not included in the CAD geometry. The pins thermal power is represented by a heat source added to the CFD model. A radial restriction in the heat source that drops to zero before touching the wall is applied.

The heating in the FPS active part is defined by means of a constant density volumetric heat source of 450 kW corresponding to a temperature difference of 90°C, and at FPS inlet temperature T = 400°C. The hydraulic resistance caused by the pins is accounted for in the model by means of porous media.

The HCSG with the secondary side tubes is not physically present in the model, and to model the pressure losses a porous media approach is used. The cooling in the Steam Generator (SG) is obtained by setting a sink term in the energy equation. The SG heat sink is performed with a two parameters volumetric sink [14] bringing the primary coolant temperature to the secondary fluid temperature (T_0, first parameter) in a given characteristic time (τ, second parameter): $s = \rho c_p (T_0 - T)/\tau$, with ρ density and c_p specific heat of the primary coolant. The secondary temperature is $T_0 = 380$°C and the characteristic time is $\tau = 10$ s, set to fulfil the heat balance at the FPS inlet temperature T = 400 °C and to remove about 440 kW.

The pump suction and impeller are not included in the model. Only the pump case is represented by means of a simple cylinder. To represent the action of the pump, a volumetric momentum source is set in a small length (0.5 m) region retrieved from the pump body above the riser outlet. The momentum source is tuned in order to get the desired LBE mass flow rate of 35.2 kg/s.

The insulation in the Riser is added as a solid region. The steel and the gas layers are simulated together as a single physical body. The total thermal resistance is defined by means of an equivalent thermal conductivity. The same procedure is applied in the dead volume air gap, treated as a ″solid″ gas. The radiative heat flux in this layer is modelled as an increased conductivity.

For the discretization of the geometry, the trimmed mesh model is used. A base size of 0.04 m is given, with a target size of 0.02 m and a minimum size of 0.002 m. The total volume mesh representation consists in 4.9 M cells. The Navier-Stokes and energy equations are numerically solved with RANS models in order to obtain the flow and the temperature fields. Turbulence k-ϵ realizable Two-Layer model with All y+ wall treatment is used in steady state setting.

The THETIS test section numerical model is run and the thermal equilibrium is quickly reached. The temperature and velocity fields are illustrated on vertical sections across the domain in Fig. 2. The vertical profile of the temperature in the plenum on the four chosen TC lines is shown in Fig. 3. The 0 m depth corresponds to the top of the vessel (cover level), the depth of 8.2 m being below the FPS inlet. The thermal stratification occurs mainly in the FV region, which loses a high amount of heat (110 kW).
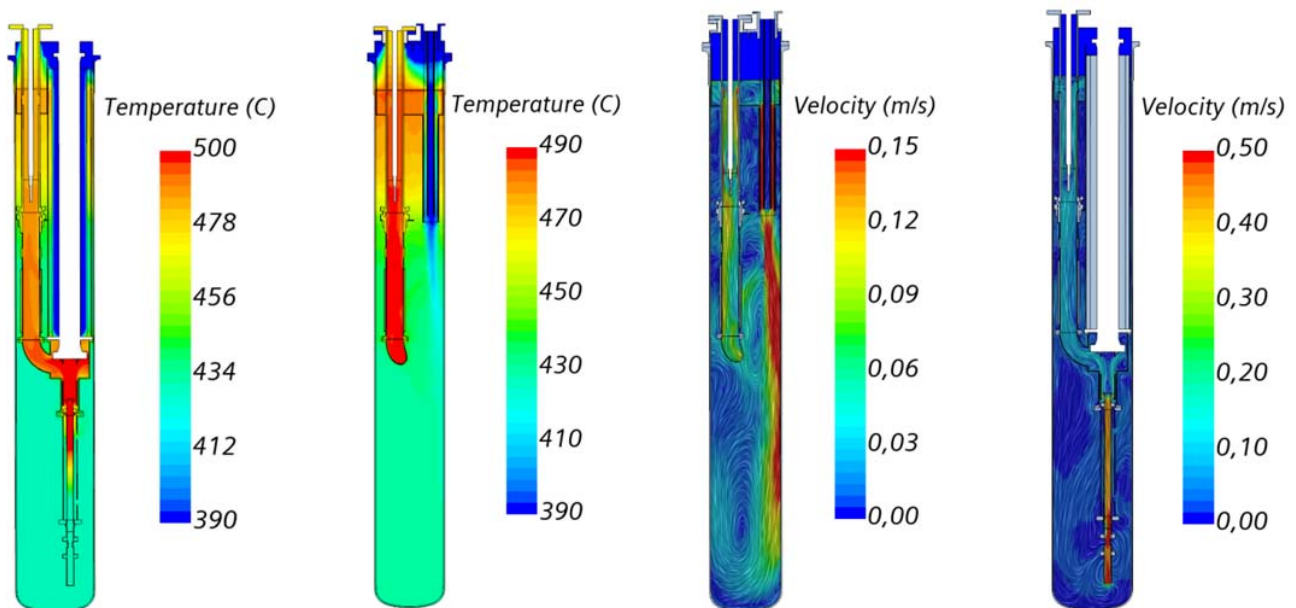
Fig.2 Steady-state preliminary results in the THETIS model, temperature and velocity fields

Since the amount of heat lost by the fitting volume is quite high, a virtual insulation is defined at its interface with the plenum, similarly as in the Riser. Based on an increased thermal conductivity scaling with the power three of the temperature, an extra thermal resistance is given. The heat loss drops from 110 kW to 10 kW. With the FV insulation implemented, the heating from the SG outlet to the FPS inlet drops from 26 K to 6 K.

The horizontal thermal stratification that encompassed all the central and upper part of the plenum, mainly driven by the FV losses, is now shifted more in the upper part and the plenum is colder by 20 K in the bottom part and by 5 K in the upper part, as indicated by the temperature field plotted in Fig. 3.
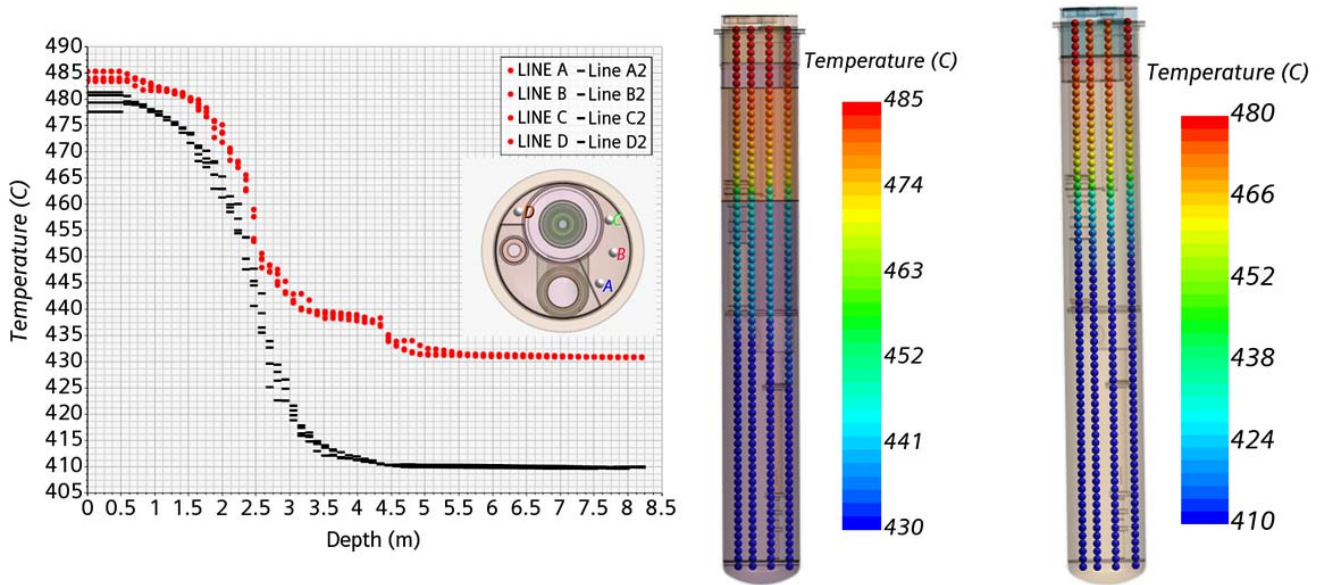
Fig. 3. Thermal stratification in the plenum along four TC lines before FV insulation (red lines) and after FV insulation (black lines). Temperature vertical profile before and after FV insulation

RVACS and vessel insulation implementation. Thermal radiation effects

Initially, the vessel was considered adiabatic, but since important heat losses are expected, external insulations are added with different widths for the upper and the bottom parts of the vessel, and appropriate thermal boundary conditions are defined: convection thermal specification with temperature 40ºC. The cover is considered insulated as the rest of the vessel, but the effective insulation is not included. Ambient temperature of 40ºC and heat transfer coefficient are given to the cover external walls: h = k/l = 0.31 W/m²·K. The vessel heat losses to environment are about 4.5 kW.

For the foreseen transients, the RVACS component is included in the model (illustrated in Fig. 4).

In order to perform transients, two inlet and two outlet tubes are foreseen. In steady state, it is considered a closed loop with a gap of 100 mm and an exchange length of 2750 mm. In the RVACS, stagnant air with temperature dependent density is used. Most of the RVACS surface is covered by the vessel's top insulation. For the non insulated parts (bottom ring, inlet and outlet tubes), suitable thermal boundary conditions are given: ambient temperature 300 K, and an approximated heat transfer coefficient, based on a steel layer of 2 mm wrapping the external insulation. The heat transfer coefficient is taken at h = 5 W/m²·K, a typical value in similar conditions. The RVACS contribution to the heat losses is about 3 kW. Similar thermal BCs are given to the cover external connections, resulting in 1 kW of heat losses. The overall heat losses from the vessel are about 8.5 kW.
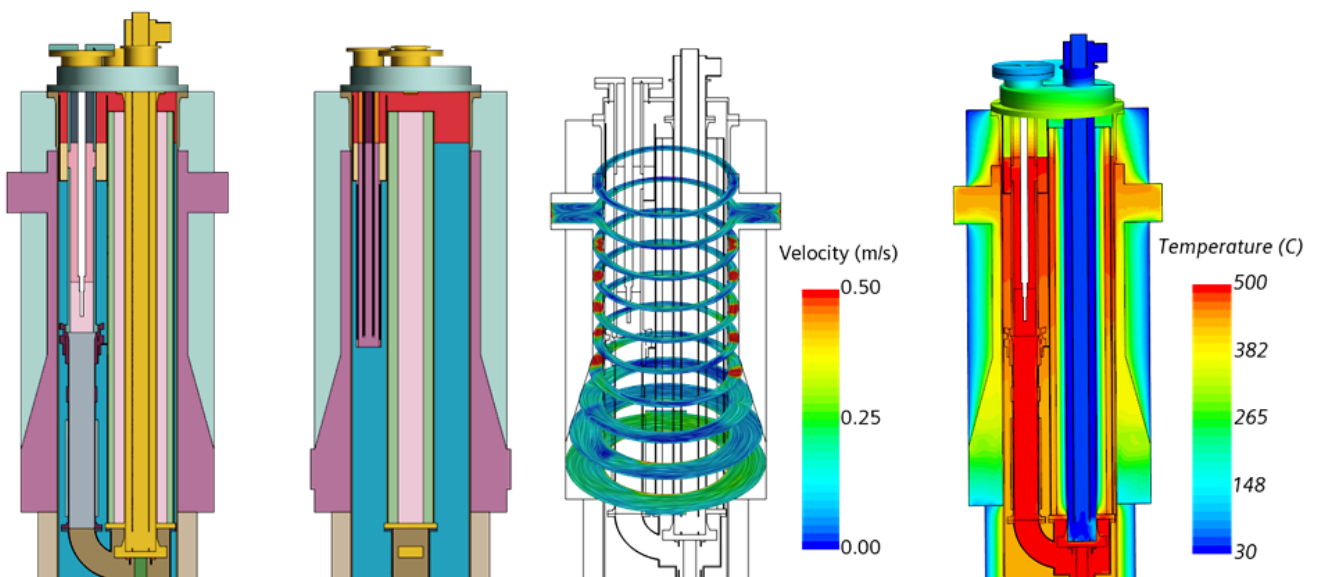
Fig.4. Details of the RVACS: Geometry, velocity and temperature fields

Based on the previous experience with radiative heat losses modeling [15, 16], it was decided to consider the thermal radiations since they were expected to give an important contribution to the heat losses. The Thermal Radiation Model is activated therefore in the cover gas (Argon with temperature dependent density), in the RVACS loop and in the Dead Volume. The following parameters are specified: LBE emissivity = 0.6 on the Argon/LBE interfaces, and steel emissivity = 0.5 on the gas-steel interfaces and on the external boundaries. The implementation of the ray tracing for thermal radiations greatly increases the computational resources requirement with simulation files size increasing from 4 to 24 Gb. But, since from the lessons learned in previous numerical models it was found out that radiation losses were responsible for a large part of the total heat losses, this aspect should not be neglected. In fact, adding the thermal radiation in the RVACS brings an additional heat loss of 15 kW for a total heat loss through the RVACS of 18 kW and overall vessel heat losses of 26 kW, respectively. The activation of the thermal radiation in the Dead Volume air cooling channel increases the heat transfer from 6.5 kW to 8 kW. The total heat losses of 34 kW is thus in line with the heat losses experimentally measured in previous campaigns.

For a better understanding of the model, a series of pictures are shown in Fig. 5, as follows: overall geometry including the insulation layers and the RVACS is shown in picture i); temperature field in the complete model before and after the FV insulation is illustrated in pictures ii) - iii); temperature and velocity fields in the model including the thermal radiations are illustrated in pictures iv)-vi).
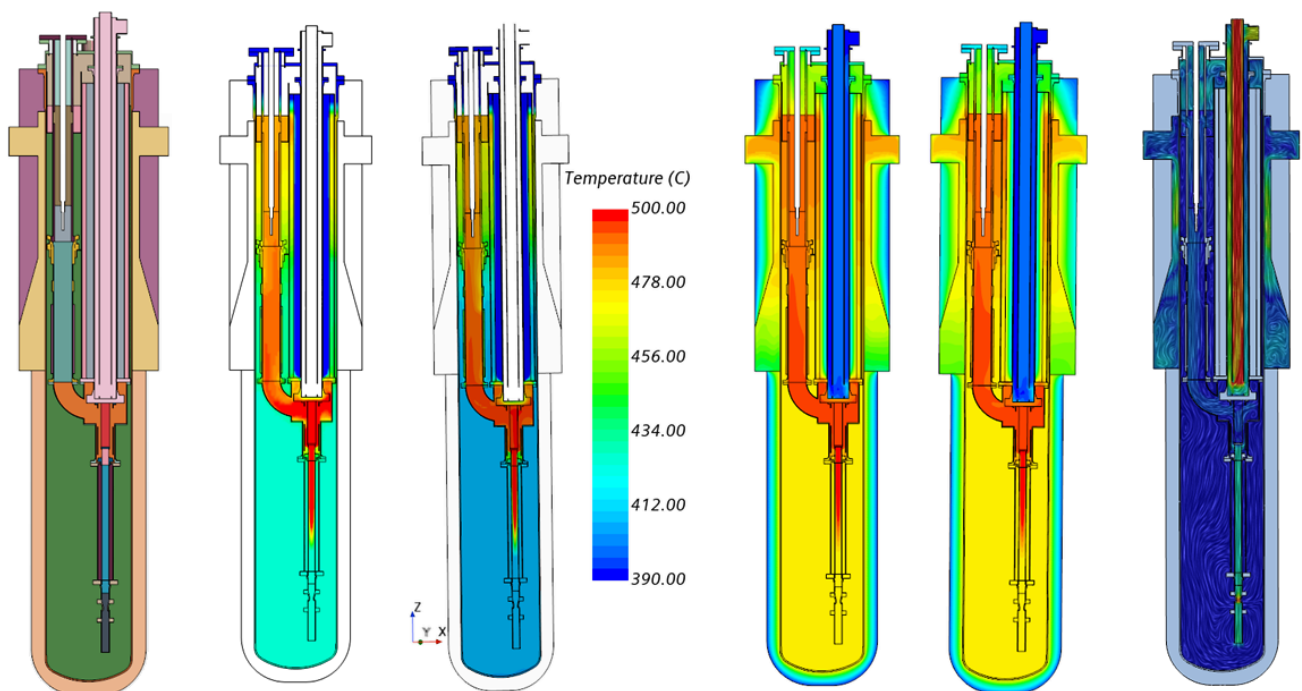
Fig.5. Complete geometry (i), plenum temperature before and after FV insulation (ii-iii), plenum temperature with thermal radiation and external temperature 40 ºC (iv), experimental temperatures (v), velocity field (vi)

Another set of thermal boundary conditions is successively implemented. According to measurements taken by ENEA in occasion of past experiments, differentiated temperature values have been registered along the vessel. These values have been assigned along the vessel's walls in the numerical model as follows: i) T = 65ºC at the top insulation wall above the RVACS; ii) T = 150ºC at the top insulation wall along the RVACS; iii) T = 51ºC at the bottom insulation wall; iv) T = 78ºC at the RVACS bottom ring.

In the numerical model, the RVACS bottom ring is not insulated. Therefore, a thermal resistance based on a 7 cm width ″virtual″ insulation layer is applied: R = 0.11 m²·K/W. The thermal radiation is added with emissivity = 0.6. At the inlet and outlet (closed) parts of the RVACS, the environment temperature T = 24ºC and heat transfer coefficient h = 5 W/m²·K are set. With these settings, the vessel heat losses drop from 23 kW to 10 kW.

There is an obvious inconsistency between the simulated heat losses and the heat losses evaluated from the outside in their radiative and convective components: 18 kW the radiative component and 15 kW the convective one, for a total of 33 kW. The consistency is retrieved if a deprecated insulation characterization is considered: multiplying by a factor of 10 the thermal conductivity in the top insulation and by a factor of 2 the thermal conductivity in the bottom insulation, the heat losses simulated become 34 kW and, thus, get very close to the expected ones. Therefore, there is a strong concern about the integrity of the insulation which will be checked by the experimental team. The effective values of the insulator thermal conductivity, of the external heat transfer coefficient and of the radiation coefficient (emissivity) will be inferred from three dedicated experimental steady state tests at different bulk temperatures.

Conclusions

The complete CFD model of the CIRCE-THETIS test section was built and progressively improved and brought to a satisfactory steady state nominal condition. The thermal stratification was strongly controlled mainly by the conductive heat transfer across the FV.

By insulating the FV, the heat loss reduced by an order of magnitude and the thermal vertical profile noticeable changed, with the thermal excursion increased by 20 K. The external vessel insulation and the RVACS have been implemented with proper thermal boundary conditions. Radiative heat transfer through the cover gas, Dead Volume and RVACS has been simulated and it was proved that thermal radiation has an important contribution.

The simulation was brought to a stabilized steady state as a first necessary step for the future investigation of transition from forced to natural circulation with the RVACS acting as DHR, as foreseen in the experimental program. Heat losses towards the environment have been evaluated under different wall temperatures. The boundary temperatures are likely to change in an unknown way during the transient, making fixed temperature non suitable BC for the simulation. Heat fluxes must be implemented instead. For this, we still need to reach consistency between the two types of BCs at steady state.

Acknowledgments

References

[1] Tarantino, M., Martelli, D., Barone, G., Di Piazza, I., Forgione, N. (2015) ″Mixed convection and stratification phenomena in a heavy liquid metal pool″, *Nucl. Eng. Design*, Vol. 286, pp. 261-277.

[2] Martelli, D., Tarantino, M., Forgione, N. (2019) ″CIRCE-ICE PLOHS experimental campaign″, *Nucl. Eng. Design*, Vol. 355, art. ID 110307, https://doi.org/10.1016/j.nucengdes.2019.110307

[3] Rozzia, D., Del Nevo, A., Tarantino, M. (2016) ″Experimental investigation of double wall bayonet tubes performance in pool type integral test facility″, Proc. of. 16th Int. Meeting on Nuclear Reactor Thermal Hydraulics NURETH-16, Chicago, USA

[4] Lorusso, P., Pesetti, A., Tarantino, M. (2018) ″ALFRED Steam Generator Assessment: design and pre-test analysis of HERO experiment″, Proc. of 26th Int. Conf. on Nuclear Eng. ICONE26, art. ID 81824, London, England

[5] Lorusso, P., Pesetti, A., Tarantino, M., Narcisi, V., Giannetti, F., Forgione, N., Del Nevo, A. (2019) ″Experimental Analysis of Stationary and Transient Scenarios of ALFRED Steam Generator Bayonet Tube in CIRCE-HERO Facility″, *Nucl. Eng. Design*, Vol.352, art. ID 110169

[6] Castelliti, D., Hamidouche, T., Lorusso, P., Tarantino, M. (2019) ″H2020 MYRTE CIRCE-HERO experimental campaign post-test activity and code validation″, Proc. of. 18th Int. Meeting on Nuclear Reactor Thermal Hydraulics NURETH-18, art. 2-s2.0-85073733801, Portland, USA

[7] Moreau, V. et al. (2019) ″Pool CFD modelling: Lessons from the SESAME project″, *Nucl. Eng. Design*. Vol. 355, ID 110343, https://doi.org/10.1016/j.nucengdes.2019.110343

[8] Zwijsen, K., Dovizio, D., Moreau, V., Roelofs, F. (2019) ″CFD modelling of the CIRCE facility″, *Nucl. Eng. Design*. Vol. 355, art. ID 110277, https://doi.org/10.1016/j.nucengdes.2019.110277

[9] Lorusso, P., Di Piazza, I., Martelli, D., Musolesi, A., Tarantino, M. (2021) ″Design of a novel test section for the LFR development: the CIRCE-THETIS facility″, Proc. of 28th Int. Conf. on Nuclear Eng. ICONE28, art. ID 65575, virtual event.

[10] Tarantino, M., Lorusso, P., Del Nevo, A., Di Piazza, I., Giannetti, F., Martelli, D. (2021) ″Preliminary design of a helical coil steam generator mock-up for the CIRCE facility for the development of DEMO LiPb heat exchanger″, *Fusion Eng. and Design*, Vol.169, ID 112459.

[11] Siemens Digital Industry Software (2020-2021) ″STAR-CCM+ User's Guide, Releases 15 and 16″, Siemens PLM Software.

[12] Lorusso, P., Bassini, S., Del Nevo, A., Di Piazza, I., Giannetti, F., Marantino, M., Utili, M. (2018) ″GEN-IV LFR development: status & perspectives″, *Prog. Nucl. Energy*, Vol. 105, pp.318–331.

[13] Profir, M., Moreau, V., Martelli, D., Di Piazza, I., Lorusso, P., Tarantino, M. (2022) ″Numerical modelling and simulation of the CIRCE facility in the PATRICIA project″, Proc. of 19th Int. Meeting on Nuclear Reactor Thermal Hydraulics NURETH-19, virtual event.

[14] Moreau, V. et al. (2019) ″An improved CFD model for a MYRRHA based primary coolant loop″, *Nucl. Eng. Design*. Vol. 353, art. ID 110221, https://doi.org/10.1016/j.nucengdes.2019.110221

[15] Profir, M., Moreau, V., Melichar, T. (2020) ″Numerical and experimental campaigns for lead solidification modelling and testing″, *Nucl. Eng. Design*. Vol. 359, art. ID 110482, https://doi.org/10.1016/j.nucengdes.2019.110482

[16] Moreau, V., Profir, M., Melichar, T., Achuthan, N. (2022) ″Lead solidification and re-melting in a pool: experiment and CFD modelling″, Proc. of 19th Int. Meeting on Nuclear Reactor Thermal Hydraulics NURETH-19, virtual event.